Glycine receptors regulate interneuron differentiation during spinal network development

Jonathan R. McDearmid, Meijiang Liao, and Pierre Drapeau*

Centre for Research in Neuroscience, Research Institute of the McGill University Health Centre, MGH Neurology L7-132, 1650 Cedar Avenue, Montréal, QC, Canada H3G 1A4

Edited by Lynn T. Landmesser, Case Western Reserve University, Cleveland, OH, and approved April 25, 2006 (received for review June 10, 2005)

Glycinergic and GABAergic excitatory chloride-mediated signaling is often the first form of activity to emerge in the nascent nervous system and has been proposed to be essential for several aspects of nervous system development. However, few studies have examined the effects of disrupting glycinergic transmission. Here we perturbed glycinergic transmission *in vivo* from the onset of development in zebrafish and examined its impact on the formation of the locomotor circuitry. Targeted knockdown of the embryonic glycine receptor α2-subunit disrupted rhythm-generating networks and reduced the frequency of spontaneous glycinergic and glutamatergic events. Immunohistochemistry revealed a reduction in the number of spinal interneurons without affecting sensory and motor neurons. This effect was accompanied by a concomitant increase in the number of mitotic cells, suggesting that glycine receptors regulate interneuron differentiation during early development. Despite the loss of many interneurons, a subthreshold rhythm-generating circuit was still capable of forming. These data provide evidence that glycine receptors, in addition to their role in neurotransmission, regulate interneuron differentiation during development of this central neural network.

spinal cord | zebrafish | proliferation

Glycine and GABA receptors are chloride-conducting ligand-gated ion channels that mediate fast synaptic inhibition in the adult CNS. In contrast, during embryonic development these receptors are excitatory and often generate the earliest forms of electrical signaling in the immature nervous system. This signaling occurs initially via paracrine release at times preceding synaptogenesis (1–3) and subsequently via synaptically mediated patterns of immature activity at later developmental stages (4–9). Early transmitter signaling has been implicated in a range of developmental processes such as differentiation, migration, neurite outgrowth, axon pathfinding, synaptogenesis, and survival of nascent neurons (2, 3, 10–18).

Recent studies have shown that glycine receptors (GlyRs) can affect differentiation of retinal precursors (18). However, a similar role of GlyRs during neural differentiation in other CNS regions has not been examined. We have addressed this issue by perturbing embryonic GlyR α2-subunit expression from the onset of fertilization in zebrafish embryos. We examined the effects on the rhythm generation and spontaneous glycinergic and glutamatergic currents in spinal motoneurons as well as on the numbers of mitotic and postmitotic cells. Our results indicate that GlyR α2-subunits are involved in regulation of interneuron differentiation during spinal cord development.

Results

Motor Circuit Development Requires GlyRs. In vertebrates (19), including zebrafish (20–22), five GlyR subunits have been identified and are termed α1–4 and β. Using sensitive fluorescence *in situ* hybridization (23) we examined the expression patterns of the α1- and α2-subunits in the spinal cord. As can be seen from Fig. 1*A*, the GlyR α2-subunit was expressed in the embryonic spinal cord (at 1 day) whereas in the newly hatched zebrafish larva (2 days) expression was undetectable. In contrast, the GlyR α1-subunit was detected in spinal cord of larvae but not embryos.

To perturb glycinergic signaling we used antisense morpholino oligonucleotides (AMOs) (24) targeted against the GlyR α1- and α2-subunit mRNAs (22). Embryos were injected with AMOs at the one- to four-cell stage and raised to the appropriate age to study the impact on development of the spinal motor circuitry for swimming. We first used antibody staining to examine GlyR subunit expression in AMO-injected fish. Because no GlyR α2-specific antibodies are currently available we used the mAb4a antibody (25), which recognizes an epitope common to all GlyR subunits. In embryonic fish, mAb4a staining was detected in sections of wild-type and GlyR α1 knockdown fish but not GlyR α2 knockdown fish (Fig. 1*B i–iii*). In contrast, strong mAb4a staining could be detected in wild-type and GlyR α2 knockdown larvae whereas GlyR α1 knockdown larvae showed only weak staining (Fig. 1*B iv–vi*). As controls, fish were injected with mismatch α1 and α2 AMOs in which four to five bases had been scrambled. mAb4a staining in mismatch AMO-injected fish was similar to wild type (Fig. 1*B vii–x*). Coinjection of both α1 and α2 AMOs abolished all GlyR staining in the larvae (Fig. 1*Bxi*). Finally, with immunoblots we confirmed that knockdown of the α2-subunit abolishes embryonic GlyR expression. The mAb4a antibody labeled a band at the expected molecular mass (50 kDa) in wild-type and GlyR α2 mismatch embryo fractions but not GlyR α2 knockdown embryo fractions. In larvae, mAb4a labeling was detected in wild-type, GlyR α2 knockdown, and GlyR α2 mismatch fractions (Fig. 1*Bxii*), presumably because of expression of other GlyR subunits at this later stage. Taken together, these findings are consistent with a developmental switch in GlyR subunits, as in other vertebrates (26).

We next determined the effects of each AMO on glycinergic signaling in the developing embryo. In embryos, early motoneuron activity patterns comprise periodic, low-frequency (<1-Hz) bursts of depolarizing glycinergic synaptic current (27, 28) occurring in concert with a second form of periodic depolarization that is carried by electrical synapses (Fig. 1*C*) (29). We found the large early bursts of glycinergic synaptic activity were abolished in GlyR α2 knockdown embryos ($n = 5/5$; Fig. 1*D*) but not in the GlyR α1 knockdown embryo ($n = 3$; Fig. 1*E*). Injection of a control GlyR α2 mismatch AMO also did not affect embryonic GlyR signaling (Fig. 1*F*, $n = 5/5$).

To study the impact of disrupting GlyR signaling on network formation we examined motor behavior in posthatching larvae at 3 days in development. By this time the embryonic activity has been replaced by a relatively mature pattern of fast chemical

Conflict of interest statement: No conflicts declared.

This paper was submitted directly (Track II) to the PNAS office.

Abbreviations: GlyR, glycine receptor; AMO, antisense morpholino oligonucleotide; mPSC, miniature postsynaptic current.

*To whom correspondence should be sent at the present address: Department of Pathology and Cell Biology, Université de Montréal, Pavillon Roger-Gaudry N-535, 2900, Boulevard Édouard-Montpetit, Montréal, QC, Canada H3T 1J4. E-mail: p.drapeau@umontreal.ca.

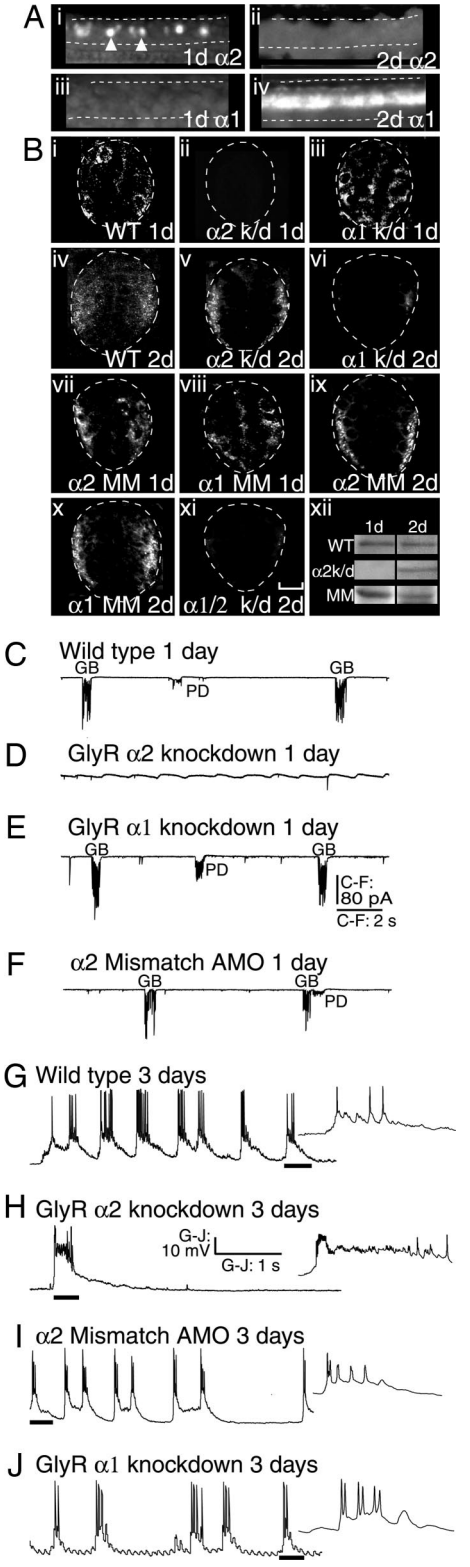

Fig. 1. GlyR perturbations during development impair motor network function. (*A*) *In situ* hybridization of GlyR mRNA transcripts in longitudinal optical sections of the spinal cord. GlyR α2 mRNA transcripts are detected at 1 day (1d α2) in development (arrowheads in *i*) but not at 2 days (2d α2; *ii*). GlyR α1 mRNA expression is absent at 1 day in development (1d α1; *iii*) and is widely expressed by 2 days (2d α1; *iv*). Broken lines demarcate dorsal and ventral limits of the spinal cord. (*B*) mAb4a-stained cryosections of embryos 24 h after fertilization reveal GlyR expression on cells of wild-type fish (WT 1d; *i*) and α1 AMO-injected fish (α1 k/d 1d; *iii*) but not α2 AMO-injected fish (α2 k/d 1d; *ii*). At 2 days mAb4a staining is increased in wild-type larvae (WT 2d; *iv*) and α2 knockdown larvae (*v*) but not α1 knockdown larvae (*vi*). mAb4a staining is observed in mismatch α2 and mismatch α1 AMO-injected embryos (*vii* and *viii*) and larvae (*ix* and *x*). Larvae coinjected with α1 and α2 AMOs have no detectable mAb4a staining (*xi*). (Scale bar: 20 μm.) (*xii*) Western blots showing mAb4a labeling in wild-type and GlyR α2 mismatch (MM) embryos (1d) and larvae (2d) and α2 knockdown (α2 k/d) larvae but not α2 knockdown embryos. (*C*) Twenty-four-hour embryo motoneuron receives glycinergic synaptic bursts (GB) and electrically mediated periodic discharges (PD; $n = 9$). (*D*) Twenty-five-hour GlyR α2 knockdown embryo reveals loss of glycinergic bursts ($n = 5/5$). (*E*) Motoneuron of a 27-h embryo injected with α1 AMO receives glycinergic synaptic bursts (GB) and electrically mediated periodic discharges (PD). (*F*) Motoneuron of a 25-h embryo injected with the GlyR α2 mismatch AMO receives glycinergic synaptic bursts (GB) and electrically mediated periodic discharges (PD). (*G*) Three-day motoneurons are rhythmically active. (*H*) Arrhythmic motoneuron activity elicited by touching in a 3-day GlyR α2 knockdown zebrafish ($n = 18/29$). (*I*) Motoneurons of 3-day fish injected with GlyR α2 mismatch AMO are rhythmically active ($n = 6/6$). (*J*) Motoneurons of 3-day fish injected with the GlyR α1 AMO are rhythmically active ($n = 51/51$). Voltage clamp holding potential in *C–F* was −60 mV. *Insets* in *G–J* depict enlarged portions of traces underlined with bars.

synaptic drive that is sufficient to generate swimming behavior (30) (Fig. 1*G*). When motoneuron activity in GlyR α2 knockdown larvae was studied either no activity at all ($n = 11/29$) or large, transient depolarizing potentials were observed ($n = 18/29$; Fig. 1*H*). The GlyR α2 knockdown phenotype could be mimicked by raising embryos in the GlyR antagonist strychnine (100 μM; $n = 14/14$). Injection of the GlyR α2 mismatch AMO did not affect rhythm generation (Fig. 1*I*). Furthermore, injection of the GlyR α1 AMO also did not perturb rhythmic motoneuron activity ($n = 51/51$; Fig. 1*J*).

GlyR Perturbation Reduces Synaptic Activity. To further examine the spinal network in GlyR α2 knockdown fish, we first recorded sensory (touch)-evoked potentials in motoneurons of 3-day larvae. In wild-type larvae these received barrages of evoked synaptic potentials ($n = 5/5$; Fig. 2*A*) whereas GlyR α2 knockdown larvae did not ($n = 9/9$; Fig. 2*B*). We next determined the state of individual synapses by recording miniature postsynaptic currents (mPSCs) after block of action potentials with tetrodotoxin. Glycinergic mPSCs were isolated in wild-type motoneurons ($n = 11$; Fig. 2*C*) and in motoneurons of GlyR α2 knockdown fish at 3 days ($n = 10$; Fig. 2*D*). These mPSCs presumably arise from GlyRs composed of subunits other than GlyR α2, such as GlyR α1 (see Fig. 1*A*). Analysis of the mPSCs in GlyR α2 knockdown larvae (Fig. 2*G*) revealed a small but significant increase in peak conductance and a large decrease in the frequency of occurrence with no difference in either the rise times or decay durations. When glutamatergic mPSCs were isolated in wild-type larvae (Fig. 2*E*) and GlyR α2 knockdown larvae (Fig. 2*F*) comparable results were obtained (Fig. 2*H*). These results indicate that disruption of GlyR α2-subunits causes a dramatic reduction in both types of synaptic events in the developing zebrafish spinal cord.

GlyRs Regulate Interneuron Numbers. To determine how spinal cord transmission was reduced in GlyR α2 knockdown fish, we examined its cellular composition. We first used the pan-neuronal anti-Hu antibody, a marker for recently differentiated neurons (31). Fig. 3 *A–C* depicts anti-Hu labeling in wild-type spinal cord at 1, 2, and 3 days in development. In GlyR α2 knockdown fish (Fig. 3 *E–G* and *Q*) we observed a striking reduction in the number of Hu-positive cells by day 2 in development, an effect that persisted into day 3. Strychnine caused a similar reduction in Hu-positive cells [168 ± 16 cells per 100-μm segment in strychnine-raised fish at 2 days ($n = 5$) vs. 224 ± 17 in wild type ($n = 21$)]. The GlyR α2 mismatched AMO

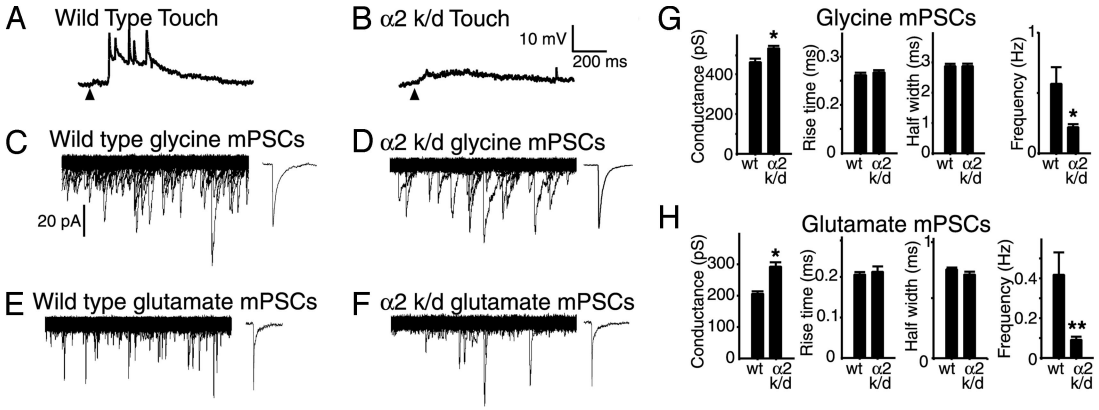

Fig. 2. Synaptic activity is reduced in α2 GlyR knockdown fish. Spinal motoneuron responses evoked by brief touches in wild-type zebrafish (*A*; $n = 5/5$) and GlyR α2 knockdown zebrafish (*B*; α2 k/d; $n = 9/9$) at 3 days in development. Arrowheads indicate onset of touch. (*C* and *D*) Glycinergic mPSCs (isolated with 1 μM TTX, 10 μM bicuculline, and 1 mM kynurenic acid) in spinal motoneurons voltage-clamped at −60 mV in wild-type zebrafish (*C*; $n = 11$) and GlyR α2 knockdown zebrafish (*D*; α2 k/d; $n = 10$). Glutamatergic mPSCs (isolated with 1 μM TTX, 10 μM bicuculline, and 1 μM strychnine) in spinal motoneurons voltage-clamped at −65 mV in wild-type zebrafish (*E*; $n = 12$) and 3-day GlyR α2 knockdown zebrafish (*F*; $n = 10$). *C–F Left* display 500 overlaps of consecutive 200-ms traces of activity. *C–F Right* display 25 averaged mPSCs for each condition. (*G* and *H*) Peak conductance, rise time, half-width, and frequency of GlyR mPSCs (*G*) and glutamatergic mPSCs (*H*) in wild-type zebrafish and α2 knockdown zebrafish (α2 k/d). *, $P < 0.01$.

(Fig. 3*D*) or GlyR α1 AMO (Fig. 3*H*) had no effect on the Hu-positive cell population [224 ± 17 in wild type ($n = 21$) vs. 227 ± 27 in mismatched AMO ($P = 0.9$; $n = 8$) and 252 ± 15 in GlyR α1 knockdown ($P = 0.4$; $n = 7$)].

We next examined whether sensory, motor, or interneuronal populations were affected in GlyR α2 knockdown fish on day 2, when the greatest relative reduction in newly differentiated spinal neurons was observed (Fig. 3*Q*). We examined sensory neurons in a transgenic line of zebrafish that express *egfp* from the promoter for neurogenin 1 (*neurog1*) (32), a basic helix–loop–helix gene expressed in zebrafish sensory neurons. In *neurog1-egfp* zebrafish, spinal cord labeling was restricted to Rohon–Beard sensory neurons that run in a column along the dorsal part of the cord (arrowheads in Fig. 3 *I–K*) and dorsal root

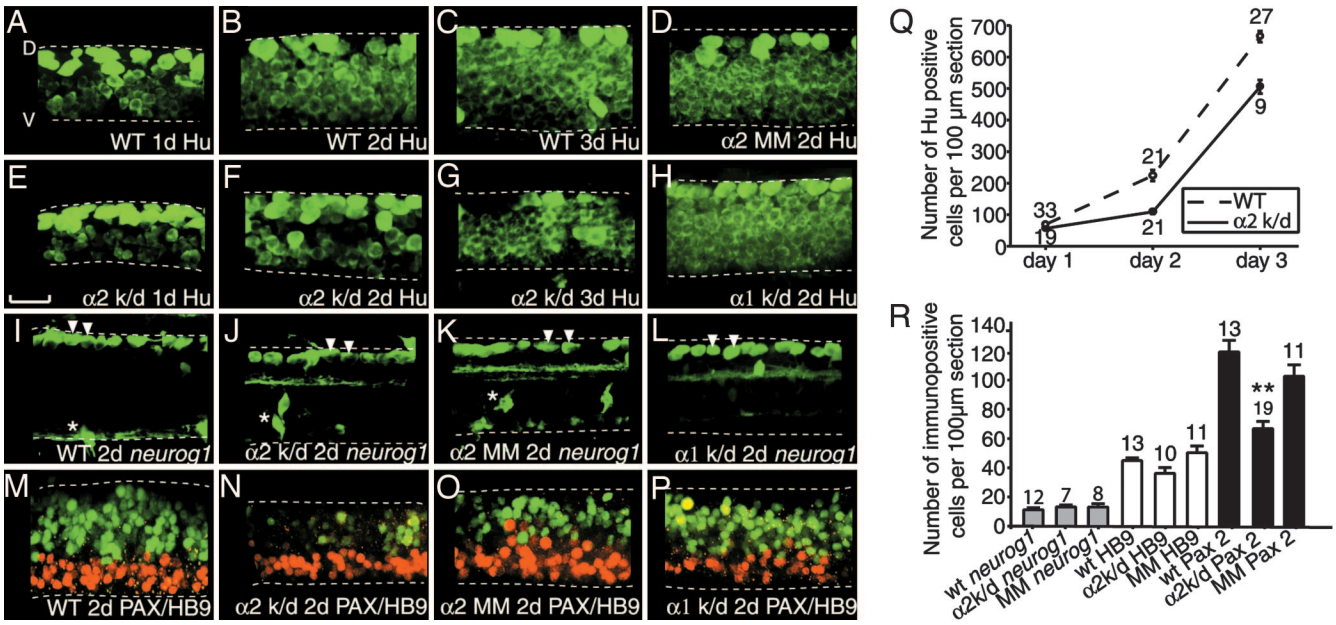

Fig. 3. Antibody staining reveals a decrease in spinal interneurons. (*A–H*) Lateral views of whole-mount zebrafish spinal cord stained with anti-Hu antibody in wild-type fish at 1, 2, and 3 days in development (*A–C*), α2 mismatch AMO-injected (α2 MM) fish at 2 days in development (*D*), GlyR α2 knockdown (α2 k/d) fish at 1, 2, and 3 days in development (*E–G*), and α1 knockdown fish (α1 k/d) at 2 days in development (*H*). (*I–K*) Anti-GFP antibody labeling of *neurog1*-positive Rohon–Beard sensory neurons (labeled with arrowheads) of wild-type (*I*), GlyR α2 knockdown (*J*; α2 k/d), GlyR α2 mismatch AMO-injected (*K*; MM), and α1 knockdown (*L*; α1 k/d) zebrafish spinal cords. (*M–P*) Lateral view of Pax 2 (green) labeling of interneurons and HB9 (red) labeling of secondary motoneurons in 2-day zebrafish spinal cord of wild-type (*M*), GlyR α2 knockdown (*N*; α2 k/d); GlyR α2 mismatch AMO-injected (*O*; α2 MM), and α1 knockdown (*P*; α1 k/d) zebrafish spinal cords. Dotted lines demarcate dorsal (D) and ventral (V) limits of the spinal cord. (Scale bar: 30 μm.) (*Q*) Graph of average number of Hu-labeled cells in 100-μm segments of spinal cord between days 1 and 3 in development for wild-type (open circles, broken line) and GlyR α2 knockdown (α2 k/d; solid circles, solid line) fish. The number of Hu-labeled neurons in wild-type fish was significantly different from GlyR α2 knockdown fish at each developmental stage ($P = 2 \times 10^{-3}$ at day 1; $P = 4 \times 10^{-5}$ at day 2; $P = 3 \times 10^{-5}$ at day 3). (*R*) Mean number of *neurog1*-labeled (gray bars), HB9-labeled (white bars), and Pax 2-labeled (black bars) cells in a 100-μm section of spinal cord for each experimental condition. *n* values from which means were taken are illustrated below (for wild type) and above (for GlyR α2 k/d) each circle in *M* and above each bar in *N*. **, $P = 10^{-7}$.

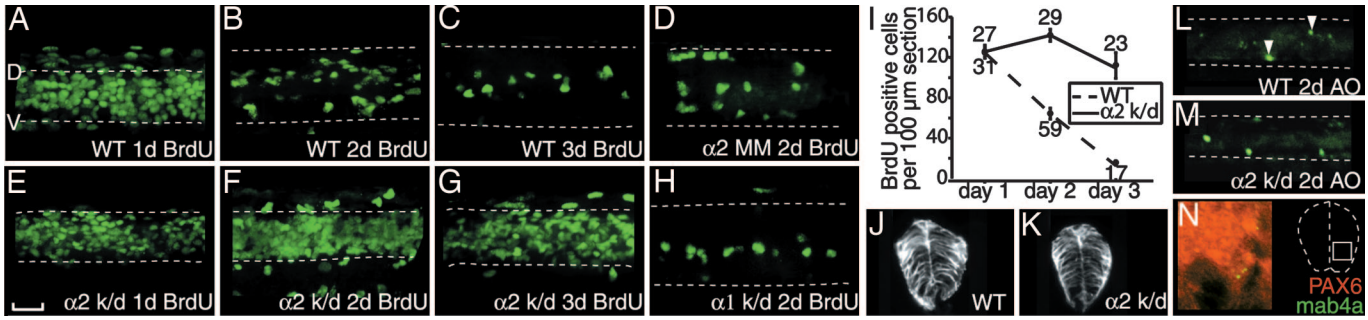

Fig. 4. Antibody staining reveals an increase in BrdU-incorporated cells in α2 knockdown fish. Shown are lateral views of BrdU-incorporated cells in whole-mount spinal cord sections of wild-type fish at 1, 2, and 3 days in development (*A–C*), GlyR α2 mismatch (α2 MM) at 2 days in development (*D*), GlyR α2 knockdown (α2 k/d) fish at 1, 2, and 3 days in development (*E–G*), and GlyR α1 knockdown (α1 k/d) fish at 2 days in development (*H*). Dotted lines demarcate dorsal (D) and ventral (V) limits of the spinal cord. (Scale bar: 25 μm.) (*I*) Graph of average number of BrdU-labeled cells in a 100-μm segment of spinal cord between days 1 and 3 in development for wild-type (open circles, broken line) and GlyR α2 knockdown (α2 k/d; solid circles, solid line) fish. The number of BrdU-labeled neurons in wild-type fish was significantly different from GlyR α2 knockdown fish at day 2 ($P = 10^{-7}$) and day 3 ($P = 10^{-7}$) but not day 1 ($P = 0.9$). The *n* values from which means were taken are illustrated below (for wild type) and above (for GlyR α2 k/d) each circle in *G*. (*J* and *K*) zrf-1 antibody labeling of radial glia in sections of 2-day wild-type (*J*) and α2 knockdown (*K*; α2 k/d) larvae. (*L* and *M*) Lateral view of acridine orange-labeled apoptotic cells (arrowheads) in wild-type (*L*) and GlyR α2 knockdown (*M*; α2 k/d) fish. (*N Left*) mAb4a (green) and PAX6 (red) costaining in a hemisomite cross section of the embryo spinal cord. (*N Right*) Diagram depicts spinal region imaged.

ganglion cells outside the spinal cord (asterisks in Fig. 3 *I–K*). The number of Rohon–Beard cells in larvae injected with the GlyR α2 AMO (14 ± 3 per 100-μm segment; Fig. 3 *J* and *R*), the GlyR α2 mismatched AMO (12 ± 2; Fig. 3*K*), or the GlyR α1 AMO (14 ± 4; Fig. 3*L*) was not significantly different from wild-type fish (12 ± 3). To examine other populations of neurons, we used antibodies to HB9, which labels motoneuron nuclei (33), and Pax 2, which labels a large subset of spinal interneurons (34). In wild-type fish, HB9-labeled cells were restricted to nuclei running along the ventral spinal cord (Fig. 3*M*) whereas Pax 2-labeled cells were restricted to a medial column of the spinal cord (Fig. 3*M*). In GlyR α2 knockdown fish, although the numbers and location of HB9-labeled cells were unaffected, a reduction in Pax 2-containing cells occurred (121 ± 9 in wild type vs. 68 ± 4 cells in α2 knockdown per 100-μm section; $P = 10^{-7}$; Fig. 3 *N* and *R*). The number of Pax 2- and HB9-labeled cells in fish injected with either the GlyR α2 mismatched AMO (Fig. 3 *O* and *R*) or the GlyR α1 AMO (Fig. 3*P*) was not significantly different from wild-type fish (Fig. 3 *M* and *R*). These findings suggest that knockdown of GlyR α2-subunits specifically affects spinal interneuron numbers during development.

GlyRs Regulate Differentiation. We next investigated the possibility that GlyR α2-subunits regulate neural differentiation in the zebrafish spinal cord. To do this, cells in S-phase were labeled with a 90-min pulse of BrdU. Subsequent immunolabeling revealed that in wild-type zebrafish the number of BrdU-positive cells was high during the first day of development and then declined between days 2 and 3 (Fig. 4 *A–C* and *I*). This finding contrasts sharply with GlyR α2 knockdown fish, where the number of BrdU-positive cells remained high throughout the same period (Fig. 4 *E–G* and *I*). Only low levels of BrdU-positive cells were observed in fish at 2 days in development that were injected with either the GlyR α2 mismatched AMO (4 ± 2 cells per 100-μm segment; $n = 9$; Fig. 4*D*) or the GlyR α1 AMO (14 ± 5 cells per 100-μm segment; $n = 9$; Fig. 4*H*). We also examined glial populations using zrf-1, an antibody that labels radial glia in the developing zebrafish, but we did not observe any obvious differences between wild-type and GlyR α2 knockdown larvae (Fig. 4 *J* and *K*).

To exclude the possibility that cell death was affecting neuronal populations, we stained spinal necrotic cells with the vital dye acridine orange (35). There was no obvious difference between the number of acridine orange-labeled cells in wild-type fish (12.5 ± 2.4 cells; $n = 6$; Fig. 4*L*) and GlyR α2 knockdown fish (10.8 ± 1.9 cells; $n = 6$; Fig. 4*M*). Because these findings suggest that impaired differentiation of spinal neurons underlies the GlyR α2 knockdown phenotype, we sought to determine whether differentiating neurons express GlyRs. Costaining of embryonic spinal cord cryosections with mAb4a and PAX6, a transcription factor involved in the specification of many classes of spinal neuron, revealed the presence of GlyRs on a proportion of PAX6-positive cells (Fig. 4*N*).

Network Activity in GlyR α2 Knockdown Fish. Because rhythmic motor activity is absent in GlyR α2 knockdown fish (Fig. 1*H*) we assumed that either the reduced interneuronal population fails to wire properly and thus a rhythm-generating network does not assemble or wiring is correct but the reduced network is too weak to generate behavior. To address this issue we took advantage of the fact that spinal locomotor circuitry can be chemically activated by NMDA (36). By using NMDA we hoped to raise the excitability of the spinal circuit and unmask a rhythm-generating circuit in the GlyR α2 knockdown spinal cord, if present. When added to whole, intact zebrafish preparations, NMDA generated repetitive bouts (each bout <2 s in duration) of depolarizing tonic drive upon which rapid (≈30-Hz) postsynaptic potentials occurred ($n = 8$; Fig. 5 *A* and *G*). Recordings from motoneurons in "spinal" fish in which the brain was removed revealed no spontaneous network activity in control conditions, but when NMDA was added a stable rhythmic drive was evoked that shared the characteristics of the activity seen in intact animals, albeit somewhat lower in frequency ($n = 10$; Fig. 5*B*).

In intact 3-day GlyR α2 knockdown fish bathed in NMDA, a slow (11.3 ± 0.4-Hz) subthreshold rhythmic synaptic drive was observed ($n = 18/21$; Fig. 5 *C* and *G*). We next looked at activity in spinal GlyR α2 knockdown fish ($n = 6$) and observed a slow, subthreshold rhythmic drive (8.1 ± 2.4 Hz; $n = 6$; Fig. 5 *D Upper* and *H*). This activity appeared to be synaptically mediated rather than arising from the voltage dependence of NMDA receptors as it persisted under voltage clamp (Fig. 5*D Lower*; $n = 3$). Furthermore, it more closely resembled that of the slow, immature synaptically mediated activity (Fig. 5*F Upper*), which also persisted under voltage clamp (Fig. 5*F Lower*) seen in intact 1-day wild-type embryos (12.8 ± 3.0 Hz; $n = 12$; Fig. 5 *E* and *G*) or spinal embryos (7.2 ± 1.3 Hz; $n = 8$; Fig. 5*F Upper* and *H*) exposed to NMDA. Taken together, these findings suggest that

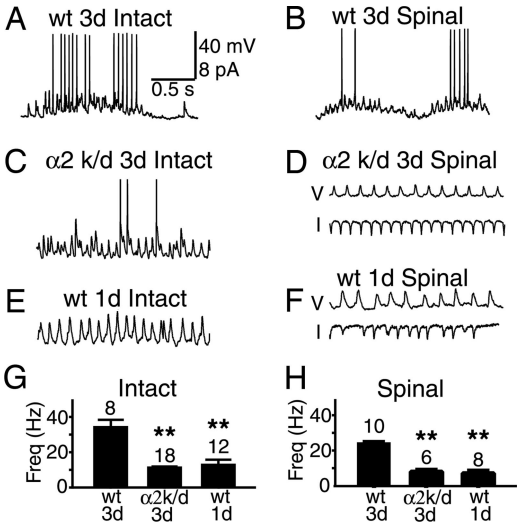

Fig. 5. Weakened spinal circuits are revealed by chemical activation in α2 GlyR knockdown fish. Voltage recordings of spinal motoneurons of 3-day fish bathed in 500 μM NMDA for intact wild-type (*A*; wt 3d), spinalized wild-type (*B*), and intact GlyR α2 knockdown (*C*; α2 k/d) zebrafish. (*D*) Voltage (V; $n = 6$) and current (I; holding potential, −60 mV; $n = 3$) recordings of a spinal motoneuron of 3-day-old spinalized GlyR α2 knockdown fish. (*E*) One-day wild-type embryo bathed in 750 μM NMDA. (*F*) Voltage recording (V; $n = 8$) and current recording (I; holding potential, −60 mV; $n = 15$) from motoneurons of a 1-day wild-type (wt 1d) spinalized embryo bathed in 1 mM NMDA. (*G*) NMDA-induced fictive locomotor frequency of intact 3-day wild-type (wt 1d), 3-day GlyR α2 knockdown (α2 k/d 3d), and 1-day wild-type fish. **, $P < 0.0001$. (*H*) Average NMDA-induced fictive locomotor frequency in spinalized 3-day wild-type (wt 3d), 3-day GlyR α2 knockdown (α2 k/d 3d), and 1-day wild-type (wt 1d) fish. *n* values from which means were taken are illustrated above each bar. **, $P < 10^{-4}$.

neuronal circuits are still present in GlyR α2 knockdown fish, but even though their synapses are mature (Fig. 2) their network activity pattern appears to be immature.

Discussion

In the current study we examined the effects of perturbing glycinergic transmission from the onset of fertilization and found that the predominant effect is to reduce spinal interneuron populations. Because this effect was accompanied by a persistently high proportion of BrdU-labeled cells, we propose that GlyRs act early in development to regulate differentiation of interneurons. There is precedence to suggest that neurotransmitters can regulate the cell cycle: GABA and glutamate have been shown to affect differentiation in the developing and adult brain (3, 13–15). Recently a similar role for GlyRs has been demonstrated during differentiation of retinal cells (18). However, the possibility that GlyRs exert similar effects during neurogenesis in other CNS regions has not been investigated. Our results indicate that a similar mechanism may affect interneuron differentiation in the zebrafish spinal cord. Thus, this effect of GlyRs may be of broad developmental significance. In the developing retina and cortex taurine is the natural ligand for GlyR α2-subunits (1, 18). Taurine does activate zebrafish GlyR α2 receptors at high (mM) concentrations (22) and is present at high concentrations in the olfactory bulb of developing zebrafish (37). Taurine is also present in the zebrafish spinal cord, although at much lower concentrations (W. C. Michel, personal communication). It remains to be established whether early glycinergic signaling in the zebrafish spinal cord depends on synaptic or extrasynaptic actions of either taurine or glycine.

Recent studies have shown that GABA-mediated signaling in progenitors of the adult hippocampus induce calcium transients and expression of a proneural gene (15), although the mechanism linking these events remains unknown. Glycine also induces elevations in intracellular calcium in the zebrafish (28), and it is conceivable that GlyR signaling underlies the spontaneous calcium transients observed during early embryonic development (38). GlyRs in the developing spinal cord may thus regulate the cell cycle in an analogous fashion to GABA in the adult hippocampus. A comprehensive analysis of gene expression profiles after GlyR perturbation will be necessary in future studies to determine how glycinergic transmission activates a neurogenic program.

Our results show that GlyRs affect differentiation of interneurons rather than motor or sensory neurons. Functional postsynaptic characteristics of individual synapses in GlyR α2-subunit knockdown fish were indistinguishable from wild type, suggesting that they had nonetheless matured normally. Our physiological data support the hypothesis that a general reduction in interneuron populations occurred because mPSC recordings indicated that both glutamatergic and glycinergic synapses were less active. Because the ratio of glycinergic to glutamatergic synapses remains close to normal (i.e., both populations are reduced by similar amounts), this result may not be as surprising as it first appears. It is well documented that disruption of the balance between glutamatergic and glycinergic activity has a dramatic effect on synapse maturation, causing homeostatic compensations that attempt to overcome the perturbation (39). We did observe a slight increase in amplitude of both glutamate and glycine mPSCs in GlyR α2 knockdown fish, which could arise from a limited attempt at homeostatic compensation for the loss of synapses, but ultimately this was insufficient to restore functional network activity.

Although the reduction of spinal neurons in GlyR α2 knockdown fish leads to a disruption of rhythm generation, a rudimentary network is still assembled in these fish, because we observed a rhythmic pattern of motoneuron activity when NMDA was applied to GlyR α2 knockdown larvae, although this pattern was of low frequency and amplitude. Hence it appears that, owing to the large reduction in the number of interneurons, functional activity is no longer generated. Indeed, a slowing of activity is predicted in models of spinal circuits when the strength of excitatory connections is reduced (40–42). Despite the impact on differentiation some interneurons were able to differentiate and indeed appeared to form elementary circuits.

In summary, our findings suggest that GlyRs can regulate exit of interneuron precursors from the cell cycle. Whether this occurs through calcium-dependent regulation of transcription factors during spontaneous embryonic activity remains to be investigated.

Materials and Methods

Details of protocols and reagents used are described in *Supporting Methods*, which is published as supporting information on the PNAS web site. Briefly, zebrafish were raised according to established procedures (43). For the GlyR α2-subunit knockdown the sequence of the AMO used was 5′-TGATAATGAGAGAGAAATGCGTCA-3′. The GlyR α1 AMO sequence was 5′-AAATAAATCCCGAGTGCGAACATTG-3′. The "control" α2 mismatch AMO sequence was 5′-TGATtATGAcAGAGtAATGgGTCA-3′, and the α1 mismatch AMO sequence was AAtTAAATgCCcAGTcCGAAgATTG. AMO injections were performed as previously described (24).

***In Situ* Hybridization and Immunohistochemistry.** Whole-mount *in situ* hybridization was performed as described previously by using the Fast Red chromogen (23). The GlyR α1 probe was targeted against the entire sequence of the RNA (44), and the GlyR α2 probe was targeted against the first 960 nucleotides of

the RNA (22). For immunohistochemistry, standard protocols were used (43).

Electrophysiology. Embryos and larvae were prepared for physiological recording as previously described (45).

Analysis. Physiological analysis was performed by using PCLAMP 8, except for mPSC analysis, which was performed by using AXOGRAPH 4.4 (Axon Instruments). For cell counts, 100-μm longitudinal spinal cord sections were imaged in z-series (at 3 μm apart) throughout the entire transverse plane of the spinal cord. The total number of stained cells within each entire z-series was determined by using METAMORPH imaging software (Universal Imaging). Spinal sections located at the level of the anus were used for imaging in all experiments. Student's *t* tests were used to test for significance between data sets. Data are shown as mean ± SE.

We are grateful to O. Tsatas, J. Laganiere, and F. Gros-Louis for assistance preparing cryosections. We thank C. Goblet (Institut Pasteur, Paris) for the GlyR α1 construct; C. Plessy (Univ. of Strasbourg, Strasbourg, France) for the *neurog1-gfp* transgenic fish; and K. Sillar, C. Bourque, and R. Buss for critical reading of earlier versions of the manuscript. This work was supported by a grant from the Canadian Institute of Health Research (to P.D.) and a fellowship from the McGill University Health Center Research Institute (to J.R.M.).

1. Flint, A. C., Liu, X. & Kriegstein, A. R. (1998) *Neuron* **20,** 43–53.
2. Manent, J. B., Demarque, M., Jorquera, I., Pellegrino, C., Ben-Ari, Y., Aniksztejn, L. & Represa, A. (2005) *J. Neurosci.* **25,** 4755–4765.
3. Liu, X., Wang, Q., Haydar, T. F. & Bordey, A. (2005) *Nat. Neurosci.* **8,** 1179–1187.
4. Sernagor, E., Chub, N., Ritter, A. & O'Donovan, M. J. (1995) *J. Neurosci.* **15,** 7452–7464.
5. Garaschuk, O., Hanse, E. & Konnerth, A. (1998) *J. Physiol.* **507,** 219–236.
6. Garaschuk, O., Linn, J., Eilers, J. & Konnerth, A. (2000) *Nat. Neurosci.* **3,** 452–459.
7. Nakayama, K., Nishimaru, H., Iizuka, M., Ozaki, S. & Kudo, N. (1999) *J. Neurophysiol.* **81,** 2592–2595.
8. Fellippa-Marques, S., Vinay, L. & Clarac, F. (2000) *Eur. J. Neurosci.* **12,** 155–164.
9. Gao, X. B. & van den Pol, A. N. (2001) *J. Neurophysiol.* **85,** 425–434.
10. Misgeld, T., Burgess, R. W., Lewis, R. M., Cunningham, J. M., Lichtman, J. W. & Sanes, J. R. (2002) *Neuron* **36,** 635–648.
11. Banks, G. B., Kanjhan, R., Wiese, S., Kneussel, M., Wong, L. M., O'Sullivan, G., Sendtner, M., Bellingham, M. C., Betz, H. & Noakes, P. G. (2005) *J. Neurosci.* **25,** 1249–1259.
12. Svoboda, K. R., Vijayaraghavan, S. & Tanguay, R. L. (2002) *J. Neurosci.* **22,** 10731–10741.
13. LoTurco, J. J., Owens, D. F., Heath, M. J., Davis, M. B. & Kriegstein, A. R. (1995) *Neuron* **15,** 1287–1298.
14. Haydar, T. F., Wang, F., Schwartz, M. L. & Rakic, P. (2000) *J. Neurosci.* **20,** 5764–5774.
15. Tozuka, Y., Fukuda, S., Namba, T., Seki, T. & Hisatsune, T. (2005) *Neuron* **47,** 803–815.
16. Hanson, M. G. & Landmesser, L. T. (2004) *Neuron* **43,** 687–701.
17. Tapia, J. C., Mentis, G. Z., Navarrete, R., Nualart, F., Figueroa, E., Sanchez, A. & Aguayo, L. G. (2001) *Neuroscience* **108,** 493–506.
18. Young, T. L. & Cepko, C. L. (2004) *Neuron* **41,** 867–879.
19. Legendre, P. (2001) *Cell. Mol. Life Sci.* **58,** 760–793.
20. David-Watine, B., Goblet, C., de Saint Jan, D., Fucile, S., Devignot, V., Bregestovski, P. & Korn, H. (1999) *Neuroscience* **90,** 303–317.
21. Imboden, M., Devignot, V. & Goblet, C. (2001) *Dev. Genes Evol.* **211,** 415–422.
22. Imboden, M., de Saint Jan, D., Leulier, F., Korn, H., Goblet, C. & Bregestovski, P. (2001) *Neuroscience* **103,** 799–810.
23. Novak, A. E. & Ribera, A. B. (2003) *Methods Cell Sci.* **25,** 79–83.
24. Nasevicius, A. & Ekker, S. C. (2000) *Nat. Genet.* **26,** 216–220.
25. Schroder, S., Hoch, W., Becker, C. M., Grenningloh, G. & Betz, H. (1991) *Biochemistry* **30,** 42–47.
26. Kuhse, J., Kuryatov, A., Maulet, Y., Malosio, M. L., Schmieden, V. & Betz, H. (1991) *FEBS Lett.* **283,** 73–77.
27. Saint-Amant, L. & Drapeau, P. (2001) *Neuron* **31,** 1035–1046.
28. Brustein, E., Marandi, N., Kovalchuk, Y., Drapeau, P. & Konnerth, A. (2003) *Pflügers Arch.* **446,** 766–773.
29. Saint-Amant, L. & Drapeau, P. (2000) *J. Neurosci.* **20,** 3964–3972.
30. Buss, R. R. & Drapeau, P. (2001) *J. Neurophysiol.* **86,** 197–210.
31. Marusich, M. F., Furneaux, H. M., Henion, P. D. & Weston, J. A. (1994) *J. Neurobiol.* **25,** 143–155.
32. Blader, P., Plessy, C. & Strahle, U. (2003) *Mech. Dev.* **120,** 211–218.
33. Tanabe, Y., William, C. & Jessell, T. M. (1998) *Cell* **95,** 67–80.
34. Mikkola, I., Fjose, A., Kuwada, J. Y., Wilson, S., Guddal, P. H. & Krauss, S. (1992) *J. Neurobiol.* **23,** 933–946.
35. Furutani-Seiki, M., Jiang, Y. J., Brand, M., Heisenberg, C. P., Houart, C., Beuchle, D., van Eeden, F. J., Granato, M., Haffter, P., Hammerschmidt, M., *et al.* (1996) *Development (Cambridge, U.K.)* **123,** 229–239.
36. McDearmid, J. R. & Drapeau, P. (2006) *J. Neurophysiol.* **95,** 401–417.
37. Sakata, Y., Olson, J. K. & Michel, W. C. (2003) *Methods Cell Sci.* **25,** 39–48.
38. Ashworth, R. & Bolsover, S. R. (2002) *Brain Res. Dev. Brain Res.* **139,** 131–137.
39. Turrigiano, G. G. & Nelson, S. B. (2004) *Nat. Rev. Neurosci.* **5,** 97–107.
40. Wolf, E. & Roberts, A. (1995) *Eur. J. Neurosci.* **7,** 671–678.
41. Dale, N. (1995) *J. Physiol.* **489,** 489–510.
42. Tunstall, M. J., Roberts, A. & Soffe, S. R. (2002) *J. Comput. Neurosci.* **13,** 143–158.
43. Westerfield, M. (1995) *The Zebrafish Book: A Guide for the Laboratory Use of Zebrafish (Brachydanio rerio)* (Univ. of Oregon Press, Eugene).
44. Devignot, V., Prado de Carvalho, L., Bregestovski, P. & Goblet, C. (2003) *Neuroscience* **122,** 449–457.
45. Drapeau, P., Ali, D. W., Buss, R. R. & Saint-Amant, L. (1999) *J. Neurosci. Methods* **88,** 1–13.